Chapter

THE APPLICATION OF ACOUSTIC EMISSION TECHNIQUE IN THE DELAMINATION OF LAMINATED COMPOSITES

Mohamad Fotouhi[1,*], Milad Saeedifar[2], Jalal Yousefi[2] and Sakineh Fotouhi[3]

[1]Advanced Composites Centre for Innovation and Science,
University of Bristol, Bristol, UK
[2]Department of Mechanical Engineering,
Amirkabir University of Technology, Tehran, Iran
[3]Department of Mechanical Engineering,
University of Tabriz, Tabriz, Iran

ABSTRACT

Fiber reinforced plastic composites are being increasingly used in engineering applications due to their high specific stiffness and strength. On the other hand, the incidence of internal defects may considerably alter the stiffness and reduce the strength and lifetime of the composites. The principal mode of failure in laminated composite materials is delamination. It can be caused by manufacturing faults or subsequent

[*] Corresponding author: Mohamad Fotouhi. E-mail: fotouhi.mohamad@gmail.com.

operational effects such as impact loads, fatigue, etc. It usually occurs within the structure and it is difficult to distinguish during the inspection. Therefore, it is not easy to detect the delamination existence and to characterize the onset and growth of it. Acoustic Emission (AE) is a capable non-destructive method to study the delamination damage. This chapter represents the application of AE method to investigate delamination of laminated composite materials in two major sections:

- Initiation of damage: Various approaches such as AE energy, AE count, AE cumulative energy, and Sentry function are described as appropriate tools to determine interlaminar fracture toughness (G_C) of composite materials. The AE results are also compared with the results of ASTM standard methods. It is shown that the G_C values obtained by the AE-based methods are in a close agreement with the ASTM results.
- Progression of damage: AE technique is utilized to predict delamination evolution curve, and to classify different damage mechanisms occurring during delamination propagation. In order to predict delamination evolution curve, two different AE-based procedures are presented. In the first method, after determining the velocity of the AE waves in the composite specimens, the position of the crack tip can be estimated using two AE sensors. In the second method, the cumulative energy of the AE signals is utilized for localization of the crack tip. A very good agreement between the AE-predicted crack length and the actual crack length verifies the accuracy of the presented procedures. Finally, wavelet packet transform and fuzzy clustering methods are used to classify the dominant damage mechanisms based on their AE signatures. Scanning electron microscopic observations from the damage mechanisms are in a good agreement with the AE-based classification results.

In conclusion, the results indicate that AE has a good performance to detect initiation stage of delamination, determining the delamination crack length, and discriminating the different types of damage mechanisms in the laminated composite structures.

Keywords: Acoustic emission, laminated composites, delamination, damage characterization.

1. INTRODUCTION

High performance laminated composites have been used in different engineering applications, such as aerospace, automotive, etc., because of their high specific stiffness and strength. However, probable damage mechanisms may degrade the long-term performance of these materials. Delamination is a particularly dangerous damage for high performance laminated composites that can be caused due to static or repeated cyclic stresses, impact, and so on. This damage reduces the strength/stiffness and consequently limits the life of composite structures [1-3].

Considerable efforts have therefore been done to characterize delamination in order to modify the performance of the structure [4-5]. Initiation and propagation of the crack are two major stages in delamination damage. Fiber/matrix interface micro damage is not observable and is harder to inspect, whereas, crack propagation is usually a macroscopic damage activity that can be regarded as the ultimate form of delamination occurring in the interlaminar zone and can be observed visually. In laminated composite materials, microscopic damage mechanisms are usually fiber breakage, interface decohesion and matrix cracking.

Acoustic emission (AE) is a promising method to monitor the microscopic damage mechanisms in delamination [6-8]. AE is commonly defined as transient elastic waves within a material, generated by the rapid release of energy within a material because of changes in local stress fields. Acoustic emission waves cover a wide frequency distribution ranges from audible frequencies to frequencies in MHz [9-10]. During delamination, AE signals originated from various sources of the microscopic damage mechanisms contain different AE signatures that can be used to find the relationship between the AE parameters and type of damage mechanisms.

This chapter discusses the application of AE method to investigate delamination of laminated composite materials in the initiation and propagation stages. AE energy, AE count, AE cumulative energy, and Sentry function are used instead of ASTM standard methods to detect the damage initiation and to determine interlaminar fracture toughness (G_C) of composite materials. In addition, AE technique is utilized to predict delamination evolution curve and to classify different damage mechanisms occurring during the delamination propagation. The results indicate that AE is a very efficient method for damage characterization of delamination and can lead to a fundamental understanding of the crack behavior.

2. EXPERIMENTAL PROCEDURE

2.1. Materials

The experimental works were carried out on specimens made from epoxy resin reinforced by carbon and glass fibers. The specifications of the specimens are listed in Table 1. The initial crack was formed by inserting a Teflon film with a thickness of 20 µm at mid-plane of the laminated composite during molding. The laminated composite specimens consisted of a rectangular shape and uniform thickness.

Table 1. The specifications of different composite specimens

Specimen	Thickness (mm)	Length (mm)	Width (mm)	Initial crack length (mm)	Layups	Fiber Type
GU-S1	5	150	25	20	$[0]_n$	Glass
GW-S1	5	150	25	20	$[\text{Woven } (0,90)]_n$	Glass
GU-S2	5	190	22	40	$[0]_n$	Glass
GW-S2	5	190	22	40	$[\text{Woven } (0,90)]_n$	Glass
GU-S3	5	180	25	40	$[0]_n$	Glass
GW-S3	5	180	25	40	$[\text{Woven } (0,90)]_n$	Glass
CU-S1	4	175	25	25	$[0]_n$	Carbon

2.2. Test Design and Configuration

Double Cantilever Beam (DCB), Mixed Mode Bending (MMB), and End-Notched Failure (ENF) test apparatus, shown in Figure 1, were used to apply the load to the specimens. In DCB setup, an upward force is applied to split end of the laminate to create Mode I. While in ENF setup, a downward load is applied to the specimen center to create Mode II. MMB is the combination of DCB and ENF. The length of the MMB lever arm can be changed to vary the GI/GII modal ratio values. The tests were carried out at a temperature of 24°C and at a constant displacement rate of 2 mm/min. The load and displacement were continuously measured and the crack length was visually recorded using a digital camera. The tests were iterated three times for each type of the specimens in constant loading conditions to check the repeatability of the results.

2.3. Acoustic Emission

An AE data acquisition system (PAC) PCI-2 with a maximum sampling rate of 40 MHz was used to record the AE signals. PAC R15 resonant-type, broadband, single-crystal piezoelectric transducers were used as AE sensors. The frequency range of the sensors was 100-500 kHz and the gain selector of the preamplifier and the threshold value were set to 40 dB. The surface of the sensor was covered with silicon grease to provide good acoustic coupling between the specimen and the sensor. The test sampling rate was 1 MHz. A pencil lead break procedure was used to calibrate the data acquisition system for each of the specimens. After the calibration step, the AE signals were recorded during the tests.

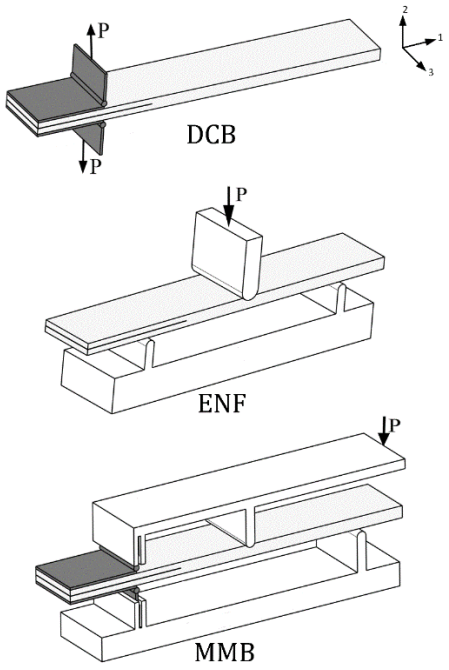

Figure 1. The boundary and loading conditions of the investigated specimens.

3. RESULTS AND DISCUSSION

3.1. Damage Initiation

In this section, various approaches such as AE energy, AE count, AE cumulative energy, and Sentry function are used to characterize the initiation stage of delamination, and to determine interlaminar fracture toughness (G_C) of composite materials. The significance of this investigation is due to the fact that initiation is a critical stage in delamination of laminated composites. Knowing the delamination behavior in initiation can lead to an enhanced design with higher strength against crack initiation. In addition to the AE-based procedures, ASTM D5528 [11] standard was also used to detect the initiation stage. The following procedures are presented in ASTM D5528 standard to determine the critical load (P_C) that is required for delamination initiation: a) Non-linearity in the load-displacement diagram (NL), (b) Visual Inspection System (VIS) and (c) The compliance increase (5% max).

Figure 2 depicts values of the P_C that are acquired from the above-mentioned methods for a GW-S1 sample.

Some researchers [2] revealed that the nonlinearity on the load–displacement plot is a practical indication of crack initiation. However, obtaining a deviation from linearity is rather difficult and this method is not completely satisfactory. Besides, visual inspection of delamination is often hard as it occurs beneath composite surfaces in actual applications [13, 14]. In this respect, AE is an effective tool for the initiation detection of delamination. A successful reliability of AE method has been reported for the damage initiation characterization by some researchers [15-17].

Two main AE-based methods for damage initiation detection in composite laminates are presented in the following sections.

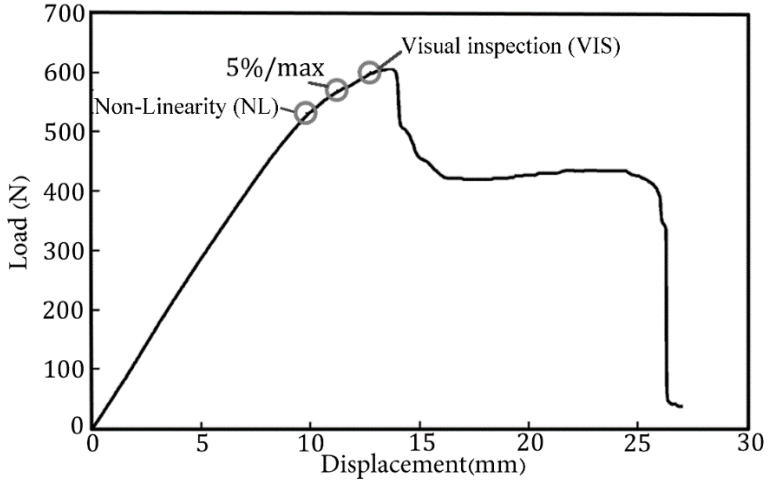

Figure 2. Pc values obtained from the ASTM standard methods for GW-S1 using ENF setup.

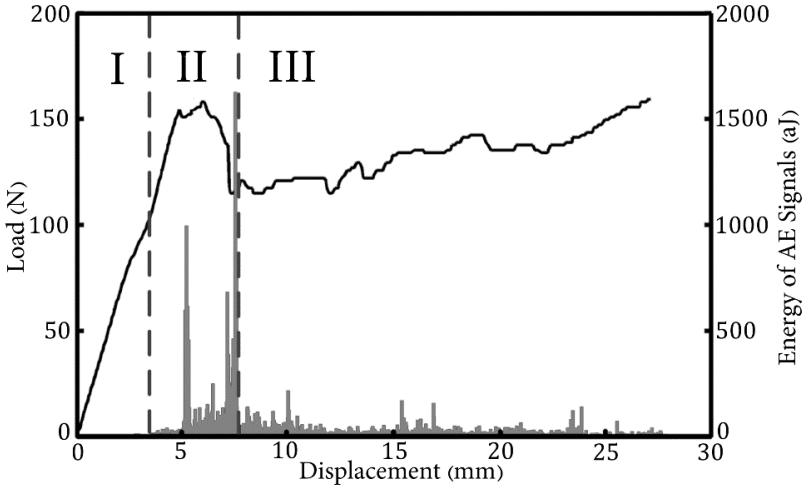

Figure 3. The energy of AE signals, during the initiation and propagation of the delamination, for GW-S1 using MMB setup.

3.1.1. Using Basic Acoustical Features Such as AE Count, AE Energy, AE Cumulative Count, and AE Cumulative Energy for Detecting the Initiation Level

Similar to the mechanical behavior of the specimens, three regions in the load-displacement curves are observable in their AE behavior. For example,

these regions are demonstrated for a typical GW-S1specimen in Figure 3. In region I, no substantial AE activity is observed. In region II, by initiation of delamination, the AE activities begin and then increase quickly. In region III, by activation of damage mechanisms and propagation of delamination, the AE activities with a medium level of energy are detected.

The distribution of AE energy and count varies during the crack propagation process. The acoustic emission energy and count distribution throughout the loading process can be used as an indicator method to predict the initiation stage of delamination. This is due to the fact that the initiation stage is a sudden phenomenon releasing high energy that corresponds to the first high rise in energy and count diagrams. The initiation stage of delamination is directly related to the P_C, the load which causes the initiation of delamination. Therefore, for identification of the P_C two methods are applied: a) energy (or count) of the AE signals and b) cumulative energy (or count) of the AE signals, which is the sum of energy or count of the recorded AE signals. In the first approach, the load at the point at which first visible high rise in the energy or count of the AE signals is observed is equal to the P_C.

Figure 4-(a) depicts the P_C acquired by the AE energy method for a typical GW-S1 specimen. In the latter technique, the load at the point at which the first surge emerges in the cumulative energy of the AE signal is equal to the P_C. Figure 4-(b) illustrates the P_C obtained by this approach for a typical GU-S1 specimen.

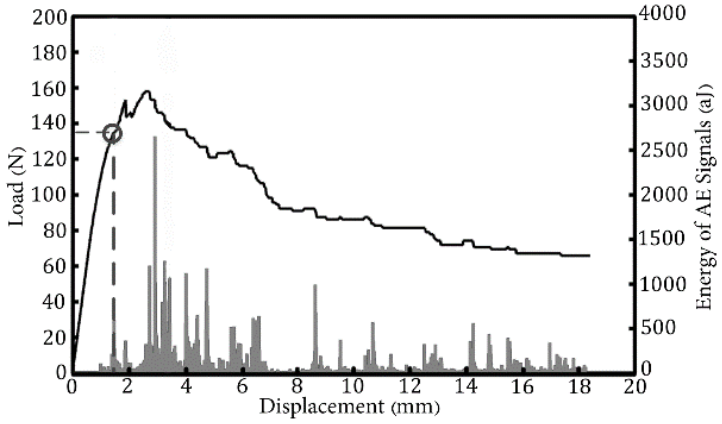

a

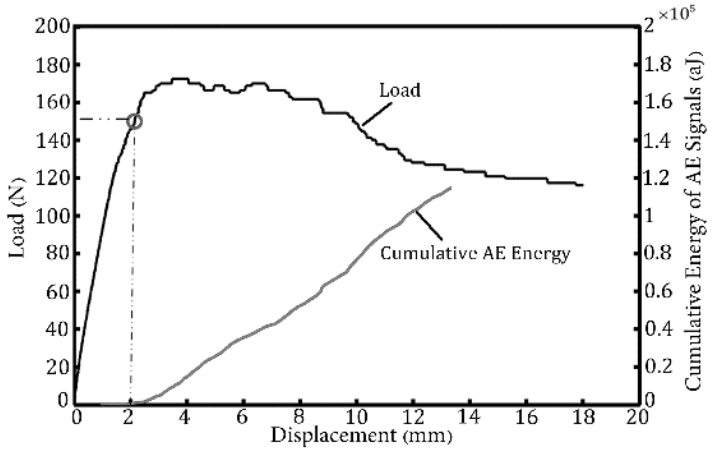

b

Figure 4. (Continued).

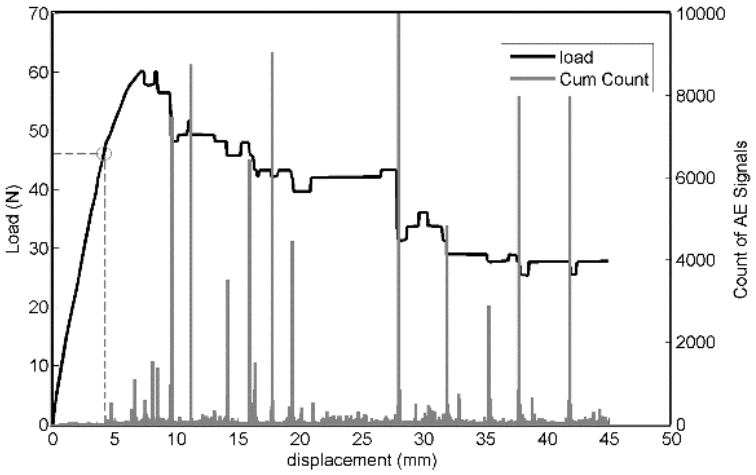

c

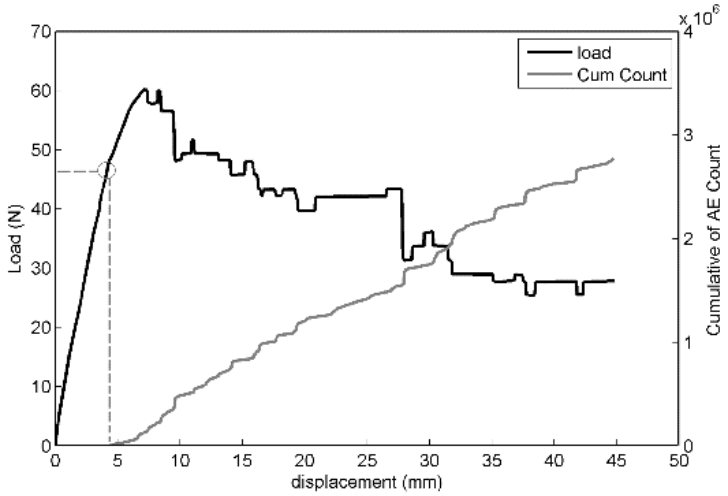

d

Figure 4. Determination of the critical load value using a) AE energy (in GW-S1) and b) the cumulative AE energy (in GU-S1) c) AE count (in GU-S3) and d) cumulative AE count (in GU-S3) approaches using DCB configuration.

Figure 4-(c) shows the distribution of the AE counts during loading for a typical GU-S3 specimen. As can be seen, before the mentioned point, no significant damage is observed and the AE counts are negligible. As the delamination initiates, the load drops off, and the AE counts surge suddenly. When this strain energy reaches to the critical strain energy that is needed for initiation of delamination, the delamination begins and the numbers of the counts grow instantly. The few weak rises in the AE count exist before the initiation of delamination that might be associated with the rubbing and elastic deformation in the specimen. In Figure 4-(d), by considering the cumulative count of the AE signals, at the initiation stage, the delamination starts to propagate as a visible high rise emerges in the cumulative counts of the AE signals. The energy needed for this stage is called critical strain energy. Before this stage, the plot is linear and all the deformations are elastic.

3.1.2. Using Sentry Function That Is a Function Relating the Mechanical and Acoustical Energies, to Obtain the Initiation Stage

In the previous section, AE information and mechanical data were applied separately for the damage characterization. The combination of mechanical data and AE information can also be implemented to have inclusive damage characterization in composite specimens. The function used for this

combination is named Sentry function. As indicated by Equation 13, Sentry function is defined as the logarithm form of the ratio of mechanical energy to acoustical energy [12]:

$$f(x) = Ln\left[\frac{E_S(x)}{E_a(x)}\right] \tag{1}$$

Where $E_S(x)$, $E_a(x)$ and x are the strain energy (mechanical energy), the AE events energy and the displacement, respectively. For computation of these energies, two reference volumes were chosen: the volume of the material where the strain energy is stored (V_1) and the volume where the delamination can propagate (V_2) and from which the AE events can take place. Thus, for the Sentry function computation, the strain energy was normalized over the V_1 + V_2 volume and the cumulative acoustic energy was normalized over the V_2 volume. Figure 5 displays the reference volumes in a DCB specimen.

Figure 6 depicts evaluation of the P_C using Sentry function method for a sample specimen. By applying the load, there is a rising trend in the stored strain energy in the specimen. The cumulative AE energy is also low before initiation of delamination (free failure domain), hence, Sentry function has an increasing trend. As the applied load increases, the ability of the material to store strain energy reaches its limits, and the AE cumulative energy significantly increases due to micro-failures appearance, so the slope of the Sentry function trend decreases. During the delamination progression, major failures take place in the specimen and there is an instantaneous release of stored energy due to the internal material failure. This key failure is defined as a significant damage level in delamination and it is in accordance with the initiation of delamination. This is shown by the sudden drop in Sentry function. The load at the point at which the Sentry function trend diminishes instantaneously is equal to the P_C.

For investigation of delamination initiation, the integral of Sentry function can also be used, as defined by Equation 2, where ΩAE is the interval at which the AE signals appear.

$$Int(f) = \int_{\Omega AE} f(x)dx \tag{2}$$

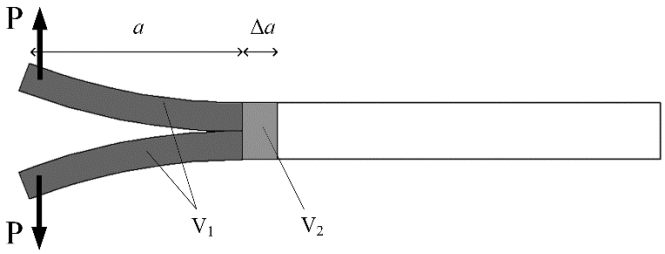

Figure 5. Schematic of the reference volumes in a DCB specimen.

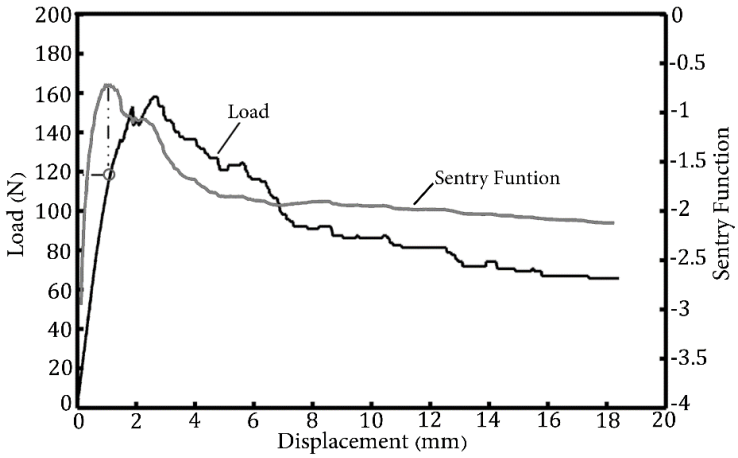

Figure 6. Determination of the critical load value using Sentry function approach for GW-S1 using DCB configuration.

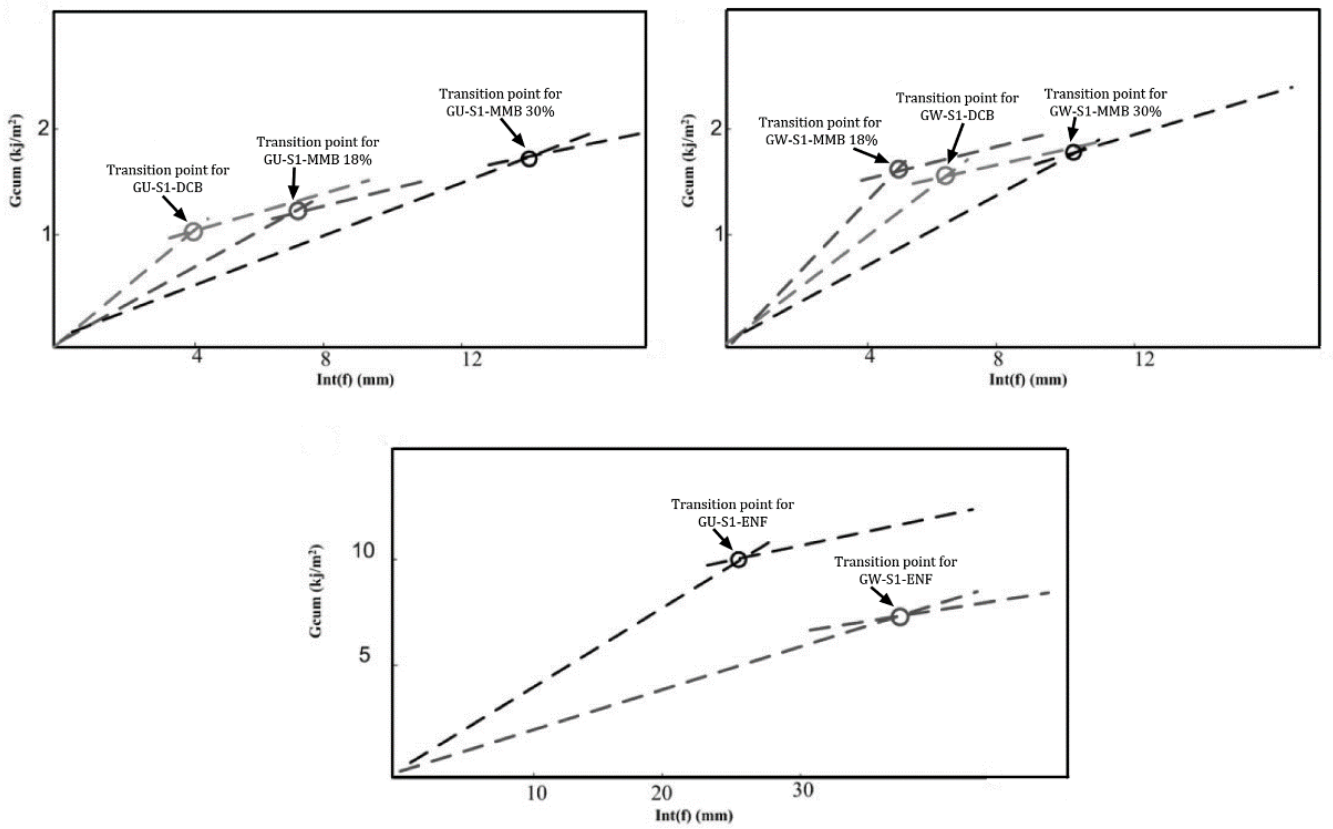

Figure 7. Plot of cumulative G versus integration of Sentry function for the specified specimens.

A distinguished bi-linear relationship between the Int(f) and G_{CUM}, by means of a linear fitting of the data, is applied to evaluate critical strain energy value (as illustrated in Figure 7). G_{CUM} is the sum of the G values computed from the obtained data during the test. Int(f) was also used as a material damage indicator and predictor for the residual strength of the composite laminates. The bi-linear relationship in Figure 7, the appearance of the transition point, is due to a variation in the material strength behavior by altering the delamination crack length. After the transition point, the slope reduces due to decreased crack propagation strength. This behavior implies that when the G_{CUM} is increased by a small amount it makes a significant increase in the Int(f). The slope of the linear diagrams before the transition point is always higher than the slope after the transition point. The slope variation is because of a change of the material strength behavior regarding the onset of delamination. Therefore, the use of the plots in Figure 7 allows evaluating the G_C values.

3.2. Progression of Delamination

Determination of the amount of delamination crack growth has a vital role in the damage tolerance analyses of the composite structures [18, 19]. In order to predict delamination growth in laminated composites, there are two main approaches; one is based on the localization of the AE signals, which is originated from the damaged area of the crack tip, and the other one is based on the AE energy released due to the delamination crack propagation.

3.2.1. Delamination Growth Prediction Using AE Signals Localization

According to the literature review [19-21], most of the damage mechanisms in laminated composites such as fiber breakage, matrix cracking, and fiber/matrix debonding occur at the small region at the crack tip, where stress is concentrated. Thus, if the velocity of AE wave in the composite material is specified, the coordinates of the crack tip can be determined using a simple AE localization method. To this aim, first, the AE wave velocity in the composite material should be specified. The velocity of AE wave in the materials is calculated according to the standard pencil lead breakage test method ASTM E976-10 [22]. The AE wave velocity in different composite materials is represented in Table 2.

Table 2. The AE wave velocity in different composite materials

Specimen	AE wave velocity (m/s)
Unidirectional Carbon/Epoxy	4937 ± 3.0%
Unidirectional Glass/Epoxy	4668 ± 1.0%
Woven (0/90) Glass/Epoxy	3380 ± 0.5%

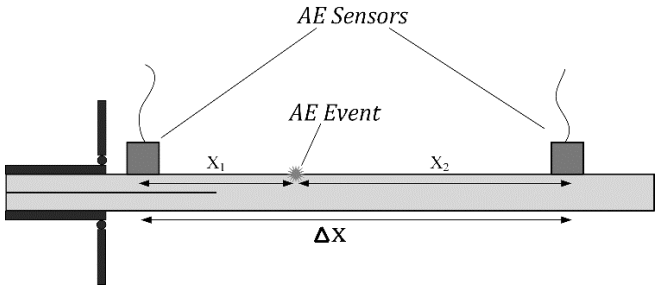

Figure 8. The schematic of AE signals localization [8].

Linear localization is utilized to predict delamination growth. In this method, two AE sensors are placed on two ends of the specimens, so that, the initial crack tip is placed between the two sensors (Figure 8). If a damage occurs in the space between the sensors, the originated AE wave reaches to the sensors at different times. This is due to the different distances of the damage from the sensors. By determining the time difference (Δt), distance between the AE sensors (Δx), and AE wave velocity (V) in the laminate, the location of the damage can be specified using Equation 3:

$$\begin{cases} x_1 + x_2 = \Delta x \\ |x_2 - x_1| = V.(t_2 - t_1) \end{cases} \quad ; \quad \Delta t < \frac{\Delta x}{V} \tag{3}$$

The delamination growth results using the localization approach are represented in Figure 9.

As can be seen, AE could predict the general trend of delamination growth, but the scattering of the AE results is too high. To reduce the scattering and increase the accuracy of the AE prediction, a new methodology was proposed. It has been shown that, in most of the laminated composites, fiber-bridging phenomena occurs at the small region behind the crack tip (see Figure 10) [23-26].

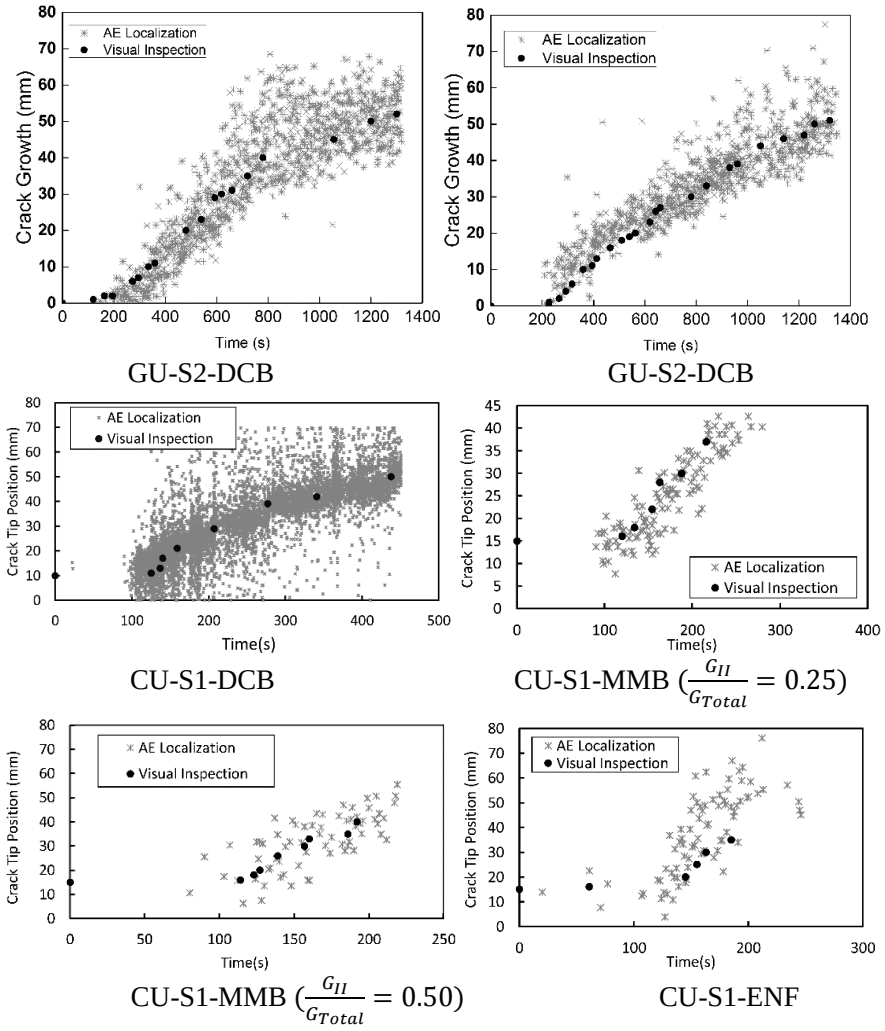

Figure 9. Prediction of delamination growth using the AE localization method.

Therefore, if the AE signals originated from the fiber breakage could be separated from the other AE signals, and the localization is being carried out using these signals, the accuracy of the AE prediction will be increased. To this aim, the fiber bundle tensile test was carried out and the originated AE signals were recorded (Figure 11). Then, the frequency range of the fiber breakage signals was specified using Fast Fourier Transform (FFT), [350 kHz-500 kHz] (see Figure 12). According to Figure 13, by eliminating the AE signals with frequency content out of this range, the scattering of the AE data

is decreased. As fiber breakage occurs behind the crack tip, the upper bound of the AE data represents the crack tip position.

However, in the specimens that no fiber bridging occurs, the last procedure cannot be used. To increase the accuracy of the AE prediction for these specimens, a new methodology is proposed. As illustrated in Figure 14, in this method, time domain of the test is discriminated to a few sections. In each section, there are a number of AE events with proprietary times and positions. All the AE signals within this section should be replaced with one AE event, which its time and position are the mean values of the times and positions of the AE events that are within the section. The appropriate number of sections is obtained by trial and error. The accuracy of the AE prediction is not changing by changing the number of sections in a great range (from 15 to 100 sections).

3.2.2. Prediction of Delamination Crack Growth Using Cumulative AE Energy

Figure 15 shows the delamination crack growth and cumulative AE energy of the unidirectional glass/epoxy DCB specimen (GU-S1).

As can be seen, the cumulative AE energy and delamination crack growth curves have similar trends. Thus, a linear relation between the cumulative AE energy and delamination crack growth can be established (Figure 16). Using this linear relation, the history of the delamination crack growth can be predicted using the recorded AE signals as represented in Figure 17.

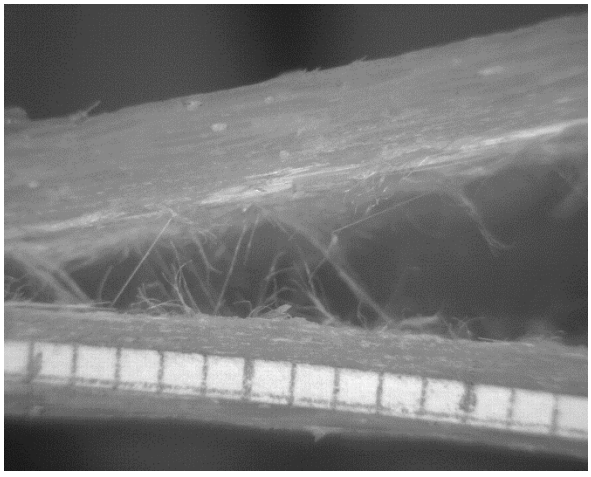

Figure 10. The fiber bridging phenomenon for GU-S1.

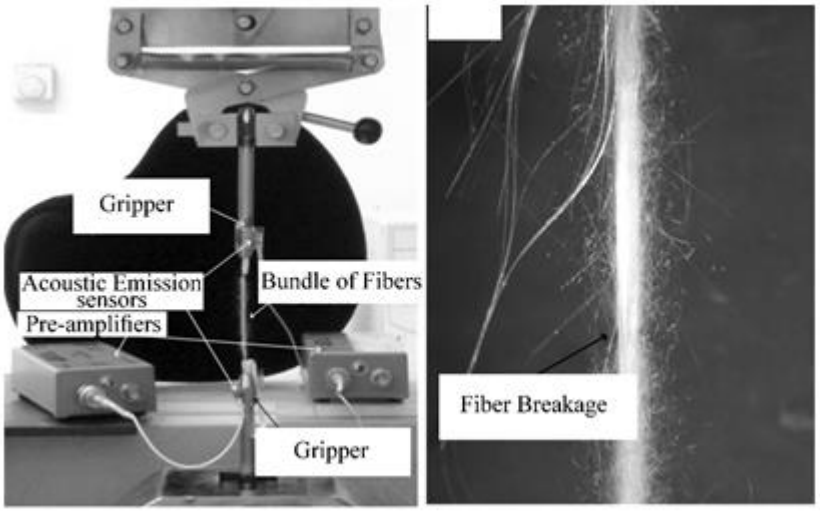

a b

Figure 11. The glass fiber bundle tensile test.

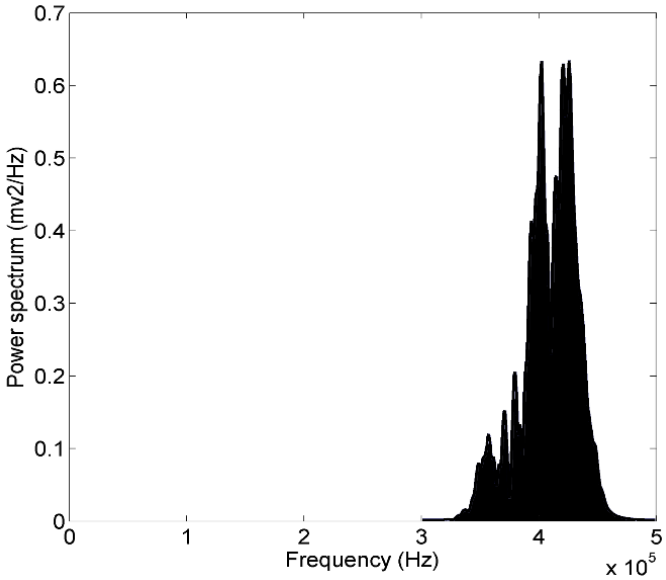

Figure 12. FFT results showing the frequency range of the AE signals obtained from the fiber bundle tensile test.

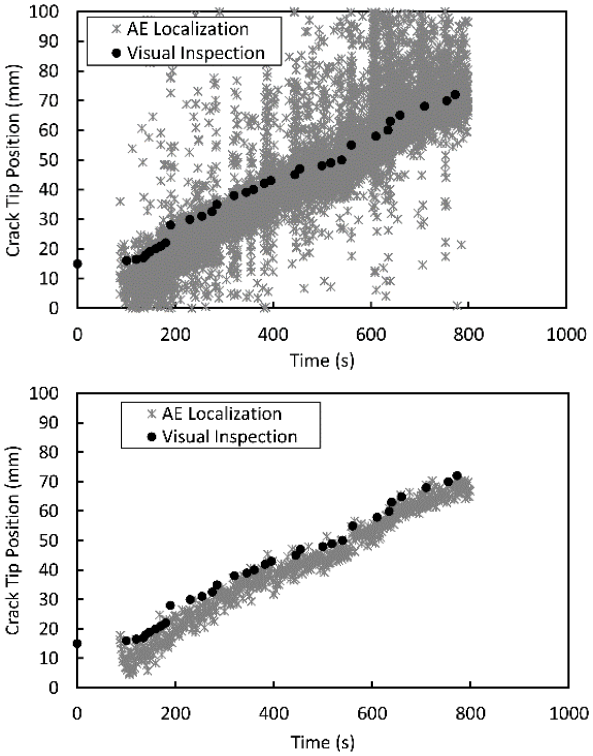

Figure 13. Increasing the accuracy of delamination growth using the AE method.

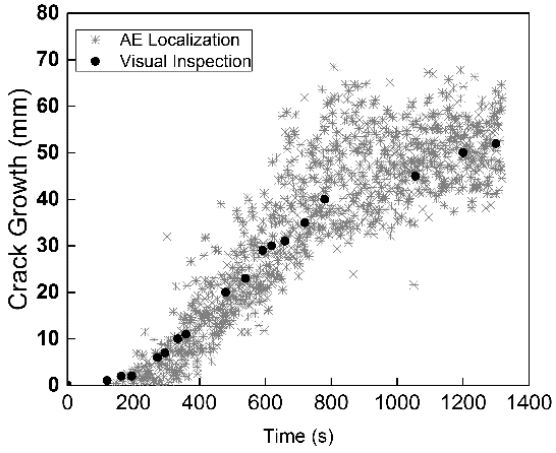

Primary prediction of AE for GU-S2-DCB

Figure 14. (Continued).

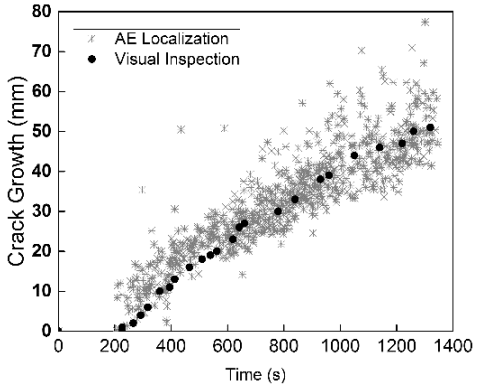

Primary prediction of AE for GW-S2-DCB

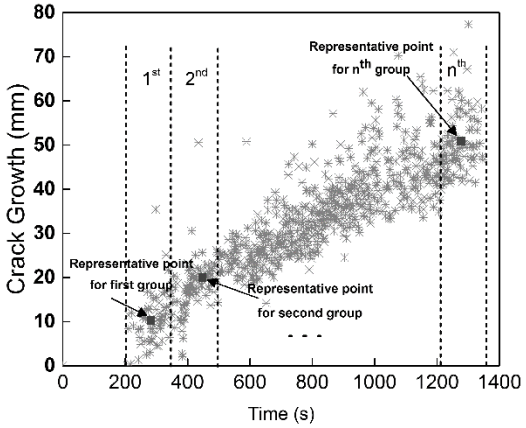

Discrete of the time domain of the test to a number of sections

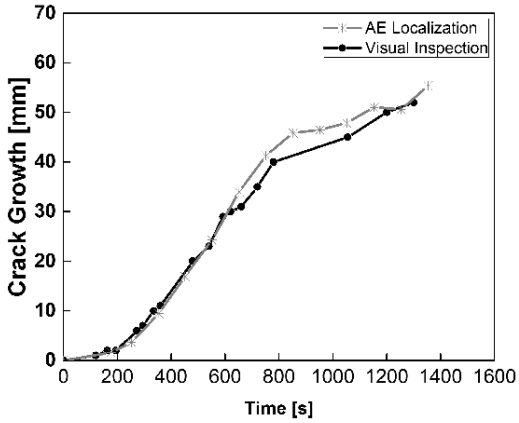

Final prediction of AE for GU-S2-DCB

Figure 14. (Continued).

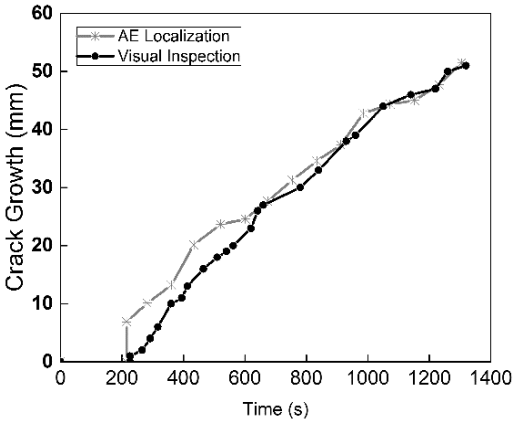

Final prediction of AE GW-S2-DCB

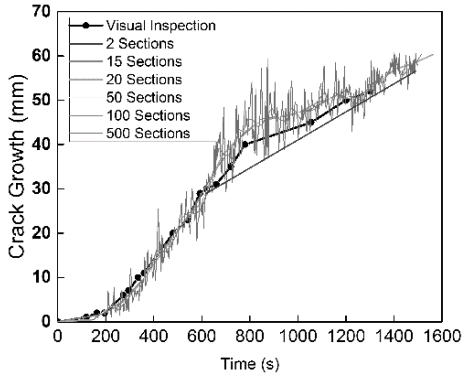

The effect of the number of sections on the predicted results for GU-S2-DCB

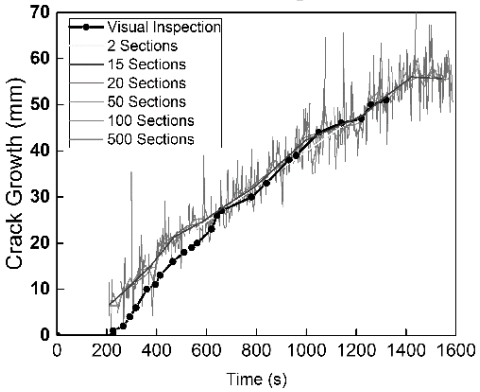

The effect of the number of sections on the predicted results for GW-S2-DCB

Figure 14. Prediction of delamination growth using AE method in the specimens without any fiber bridging.

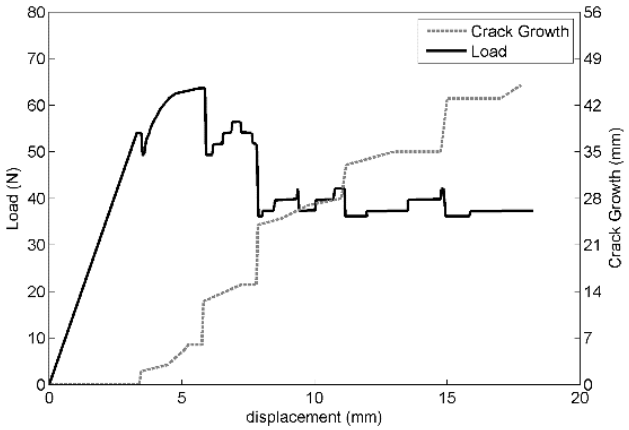

Crack growth curve (GU-S3-DCB)

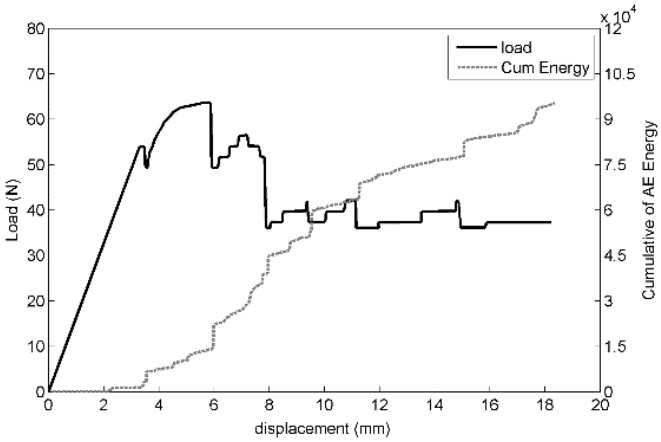

Cumulative AE energy curve

Figure 15. Crack growth and cumulative AE energy of the unidirectional glass/epoxy specimens.

In order to insure the applicability of the method under various conditions, it is also applied to measure the crack length for the carbon/epoxy composites under different loading conditions (Figure 18). The obtained results showed a very interesting consistency with the visually measured crack growth length; this is especially very useful in the case of mode II loading condition where the crack growth is unstable and hard to measure.

This method could predict delamination propagation very well, but in the early stage of the delamination growth, the method overestimates the delamination length. The reason is that, at the beginning of the crack growth,

the matrix cracking, that has a lower AE energy content, is the dominant damage mechanism. Thus, in this stage, the relation of the cumulative AE energy and crack growth is not linear (Figure 19). By progression of the delamination, other damage mechanisms such as fiber breakage and fiber/matrix debonding are activated, which have higher AE energy. Consequently, the relation between cumulative AE energy and the crack growth is close to the linear relationship. By curve fitting, it is clear that there is a power relationship between the cumulative AE energy and delamination crack growth. The proposed model could predict all stages of the delamination growth very well (Figure 20).

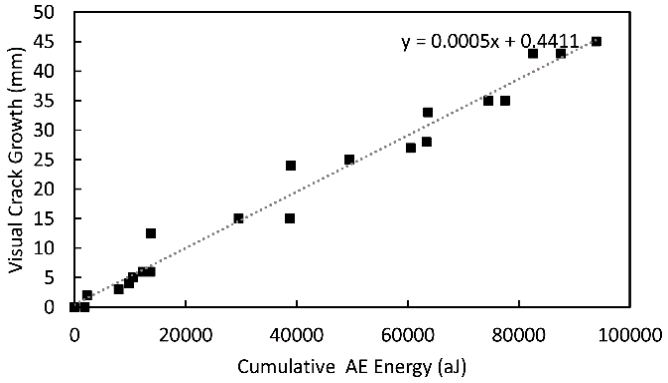

Figure 16. The linear relationship between the delamination crack growth and cumulative AE energy for GU-S3-DCB.

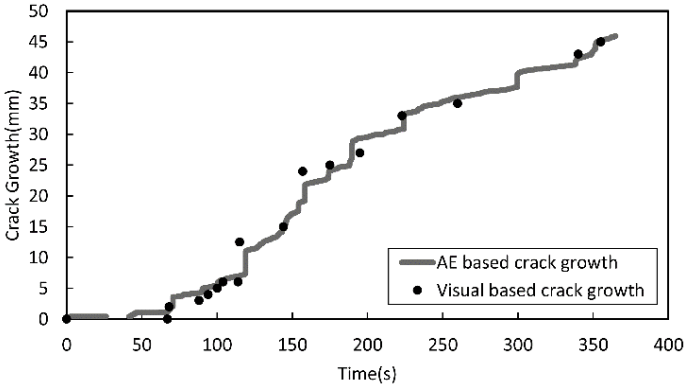

Figure 17. Prediction of the delamination crack growth using the cumulative AE energy for GU-S3-DCB.

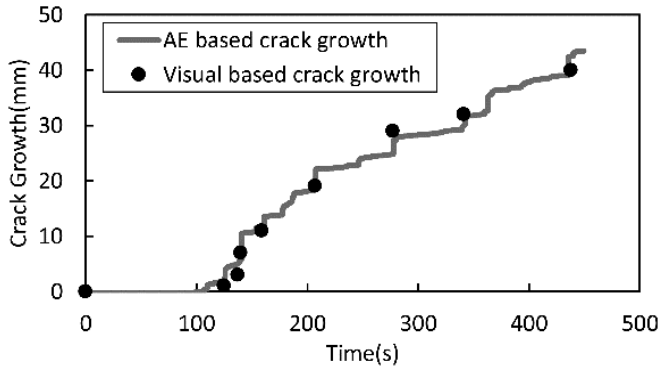

CU-S1-DCB

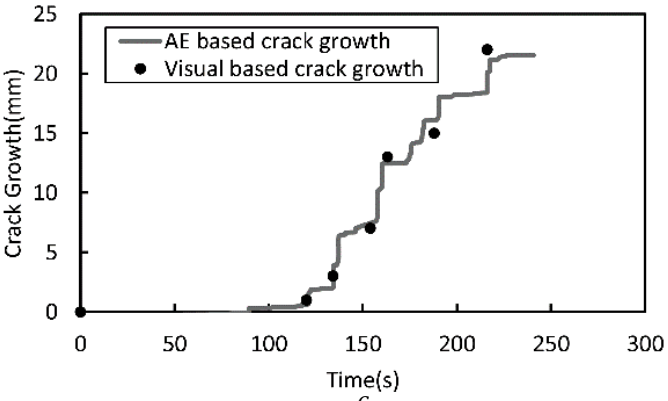

CU-S1-MMB ($\frac{G_{II}}{G_{Total}} = 0.25$)

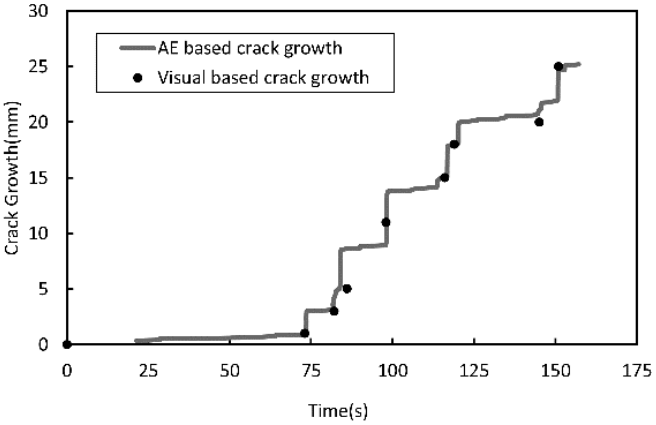

CU-S1-MMB ($\frac{G_{II}}{G_{Total}} = 0.50$)

Figure 18. (Continued).

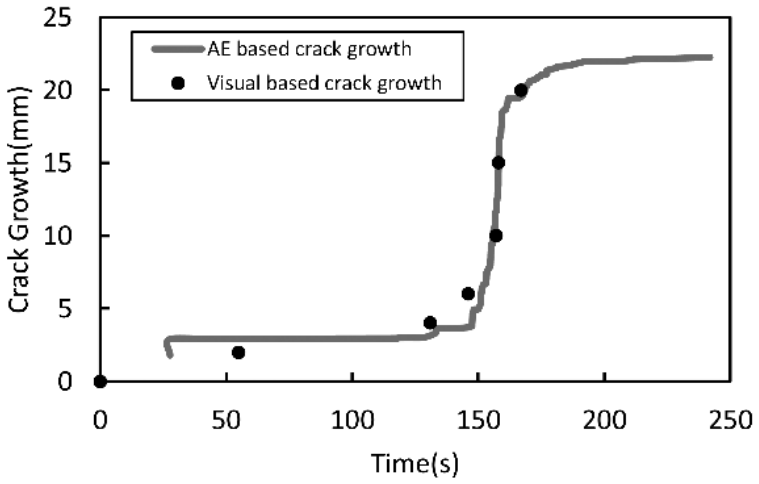

CU-S1-ENF

Figure 18. Prediction of delamination crack growth using cumulative AE energy in unidirectional carbon/epoxy specimens, under mode I, mode II and mixed-mode I&II loading conditions.

3.2.3. Damage Clustering

Wavelet Packet Transform (WPT) and Fuzzy C-Means (FCM) clustering methods are used to cluster the damage mechanisms that occurred in the specimens during delamination propagation. Prior to use of these methods, first, the AE features of each damage mechanism must be specified. To this aim, the fiber bundle and pure resin tensile tests were carried out and the AE signals of these damage mechanisms are recorded (Figure 11 and Figure 21). Then, using FFT analysis, the frequency range of each damage mechanism is specified and are utilized as AE reference patterns in the clustering procedure (Figure 12 and Figure 22). The flowcharts of the clustering procedures are presented in Figure 23.

3.2.3.1. Wavelet Packet Transform

Wavelet Transform (WT) is one of the advanced methods for signal processing. Some studies during the last decade utilized the WT as an appropriate technique for analyzing AE signals [27-29]. Fundamental and applications of WT were noted in the previous studies [30-31]. Discrete Wavelet Transform (DWT) is utilized to decompose the AE signals into some components (approximation and detail components). Mathematically, DWT is defined as:

$$f(t) = c\sum_{i}\sum_{k} DWT(i,k)2^{\frac{-i}{2}}\psi(2^{-i}t-k) \tag{4}$$

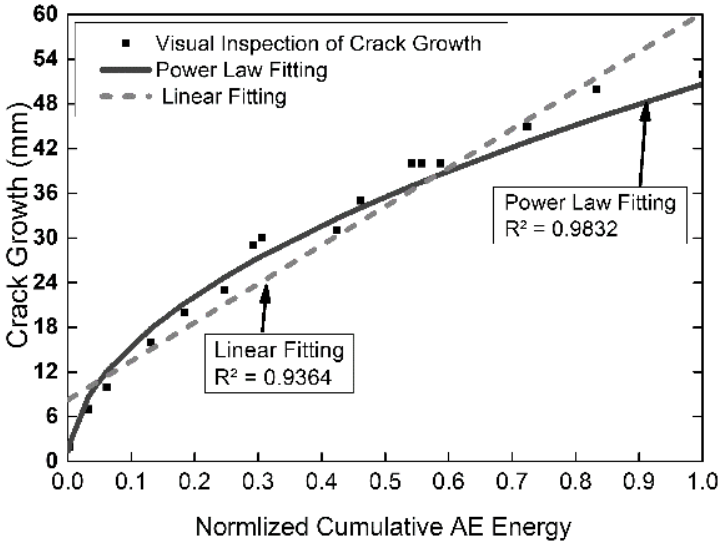

GU-S2-DCB

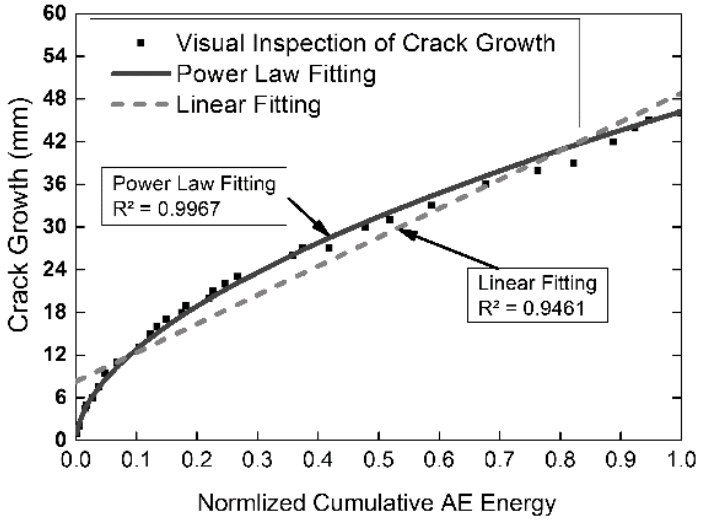

GW-S2-DCB

Figure 19. The relation between cumulative AE energy and delamination crack growth.

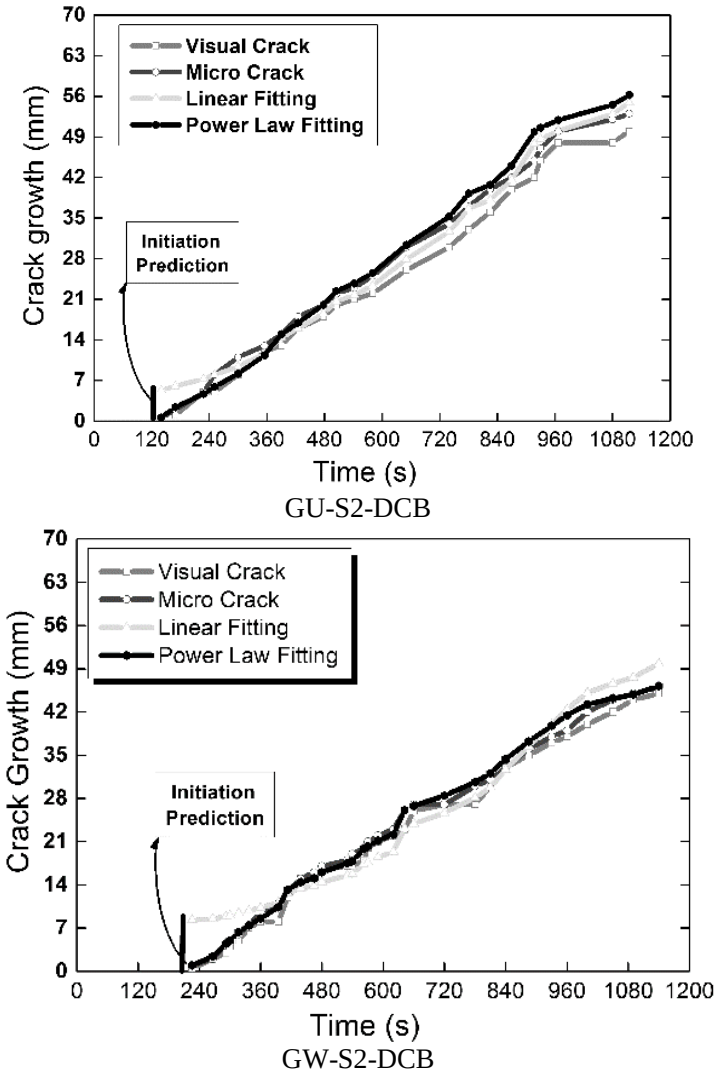

Figure 20. Prediction of delamination crack growth using linear and power relation between the cumulative AE energy and delamination crack growth.

The inverse of DWT is expressed as:

$$DWT(i,k) = \int_{-\infty}^{+\infty} f(t) 2^{\frac{i}{2}} \psi^{*}(2^{i}t - k)\,\mathrm{d}t \tag{5}$$

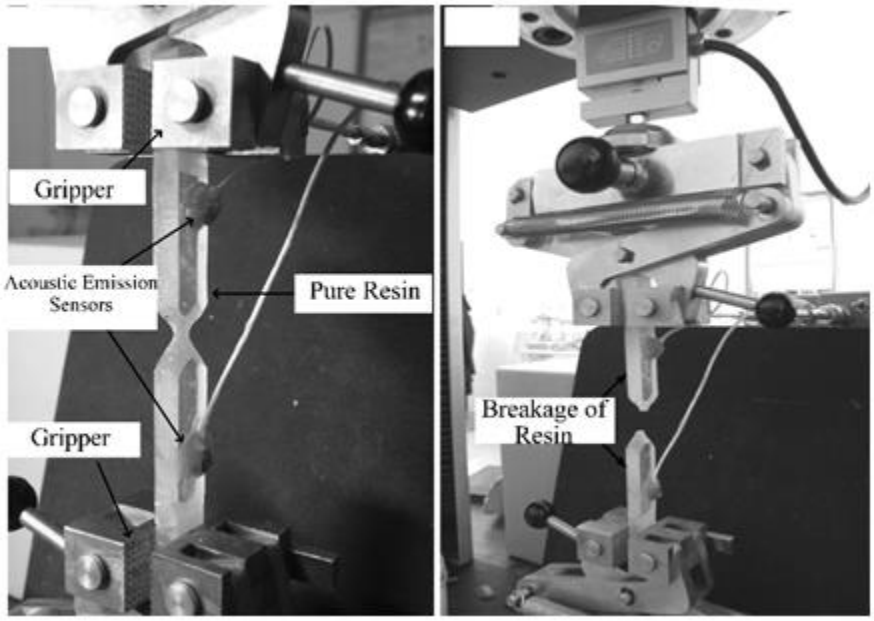

a b

Figure 21. Tensile test of the pure resin.

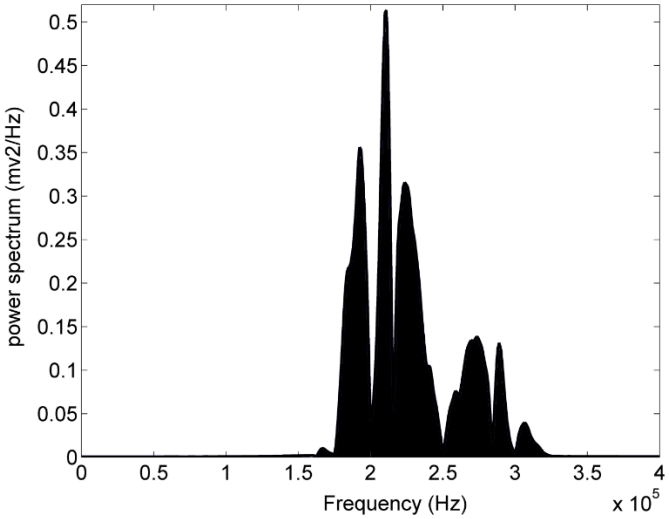

Figure 22. The frequency range of the matrix cracking obtained from FFT.

In the above relations, f(t), i, DWT (i,k), k, and ψ, are the signal that should be analyzed the decomposition level, the wavelet transform coefficients, the time domain and a mother wavelet, respectively.

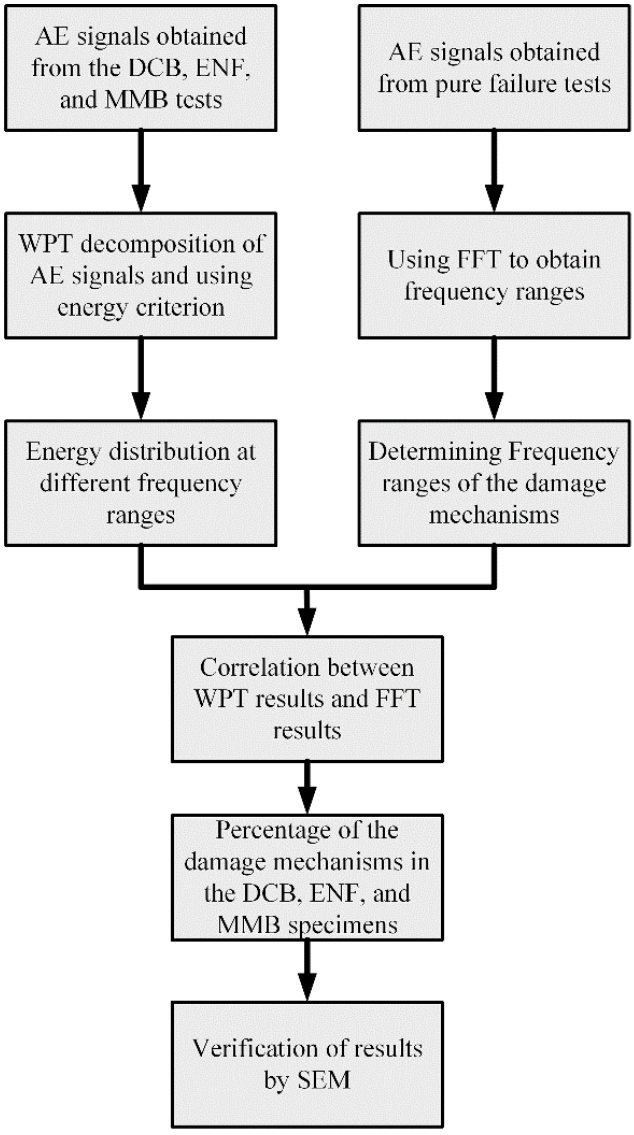

Figure 23. (Continued).

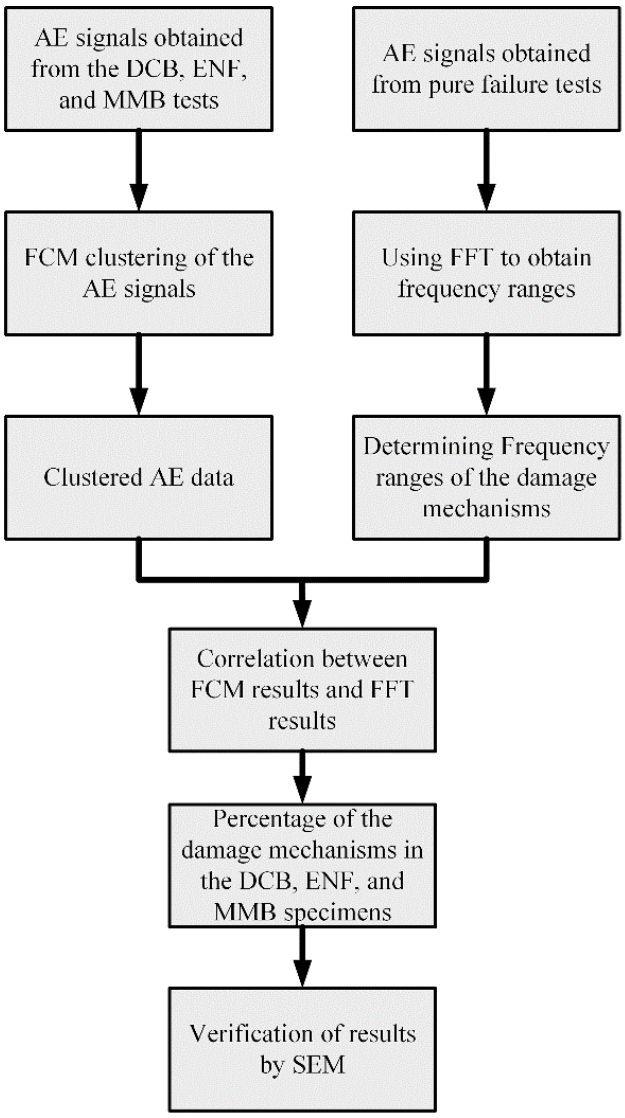

Figure 23. The flowchart of the damage clustering.

A drawback of DWT is that this method neglects the high frequency components of the AE signals during the decomposition process. Thus, some of the valuable information is eliminated [32]. To overcome this problem, WPT is utilized.

In this method, both components of the decomposed signal (the components and details) are decomposed in the decomposition process.

Wavelet packet transform is defined by $\psi^i_{j,k}$ as follow:

$$\psi^i_{j,k}(t) = 2^{-j/2}\psi^i(2^{-j}t - k) \tag{6}$$

Where i, j, and k are modulation, scale, and translation parameters, respectively.

The wavelet function ψ^i is obtained from the following equations:

$$\psi^{2i}(t) = \frac{1}{\sqrt{2}}\sum_{k=-\infty}^{\infty} h(k)\psi^i(\frac{t}{2} - k) \tag{7}$$

$$\psi^{2i+1}(t) = \frac{1}{\sqrt{2}}\sum_{k=-\infty}^{\infty} g(k)\psi^i(\frac{t}{2} - k) \tag{8}$$

Where h(k) and g(k) are the quadrature mirror filters accompanying with the scaling function and the mother wavelet function.

The wavelet packet coefficients $c^i_{j,k}$ are defined by:

$$c^i_{j,k} = \int_{-\infty}^{+\infty} f(t)\psi^i_{j,k}(t)\,dt \tag{9}$$

The wavelet packet component $f^i_j(t)$ is calculated as follows:

$$f^i_j(t) = \sum_{k=-\infty}^{+\infty} c^i_{j,k}\psi^i_{j,k}(t)\Delta t \tag{10}$$

The frequency range of each wavelet packet component is defined as follows.

The frequency range of the component:

$$[0, \frac{1}{2}f_s 2^{-j}] \tag{11}$$

The frequency range of the detail:

$$[\frac{1}{2} f_s 2^{-j}, \frac{1}{2} f_s 2^{-(j-1)}] \tag{12}$$

The energy of each component is calculated by:

$$E_j^i(t) = \sum_{\tau=t_0}^{t} \left(f_j^i(\tau) \right)^2 \tag{13}$$

In this study, to determine the energy content of each component, the ratio of the energy of each component to total energy is calculated using:

$$P_j^i(t) = \frac{E_j^i(t)}{E_{Total}(t)} \qquad i = 1,\ldots,2^j \tag{14}$$

Where $P_j^i(t)$ is the relative distributed energy.

The results of WPT for the damage clustering in the unidirectional and woven glass/epoxy DCB, ENF and MMB specimens are represented in Figure 24 and Table 3.

Table 3. Damage clustering of the DCB, ENF, and MMB glass/epoxy specimens using WPT

		Frequency ranges (kHz)		
	Specimen	187.5-250 (Matrix cracking)	250-312.5 (Fiber/matrix debonding)	375-437.5 (Fiber breakage)
Percentage of energy	GU-S1-DCB	25	20	26
	GU-S1- MMB 18%	30	26	19
	GU-S1- MMB 30%	40	18	18
	GU-S1- ENF	47	26	7
	GW-S1- DCB	35	29	8
	GW-S1-MMB 18%	36	31	8
	GW-S1-MMB 30%	38	32	7
	GW-S1-ENF	52	23	7

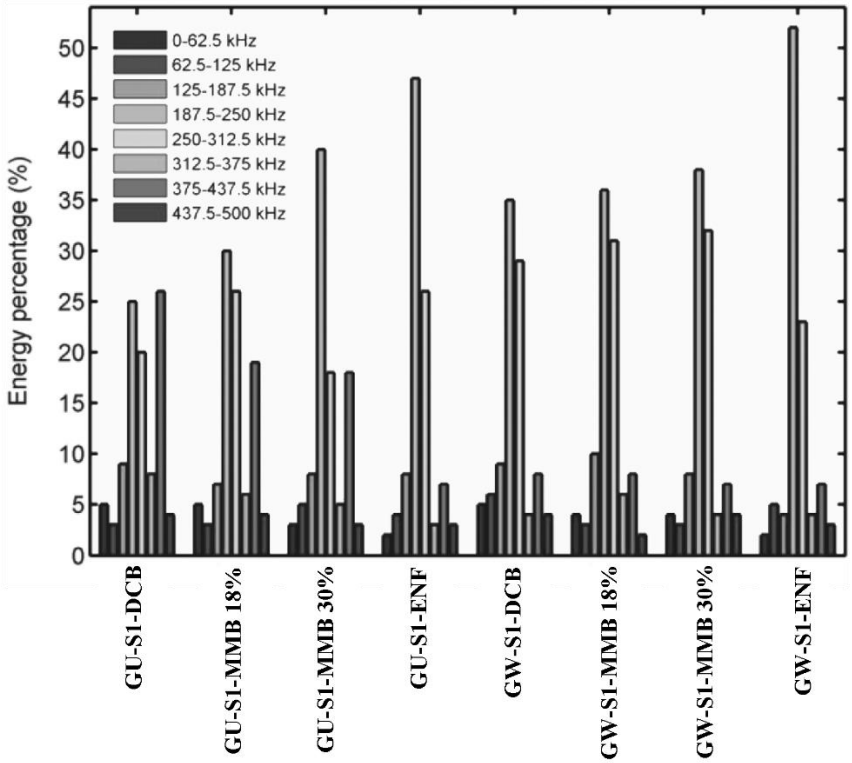

Figure 24. Damage clustering of the DCB, ENF, and MMB glass/epoxy specimens using WPT.

3.2.3.2. Fuzzy C-Means Clustering

Classifying data into groups whose members are similar in some way is defined as clustering process. Clustering methodologies are categorized into two types, including hard clustering and fuzzy clustering approaches. Hard clustering techniques comprise classical set theory and need that an object either does or does not belong to a specific cluster, but fuzzy clustering techniques permit the objects to belong to some other clusters simultaneously, with different degrees of membership between 0 and 1 [33, 34].

The data are the observations of some physical phenomena. Each observation consists of n measured variables, separated into an n-dimensional column vector $p_r = [p_{1r},..., p_{nr}]^T$. A set of m observations is denoted by $P = \{p_r | r = 1,2,..., m\}$, and is expressed as a n × m matrix [33, 34]:

$$P_{n\times m}=\begin{bmatrix} p_{11} & \cdots & p_{1m} \\ \vdots & \ddots & \vdots \\ p_{n1} & \cdots & p_{nm} \end{bmatrix} \tag{15}$$

According to membership functions, a partition can be easily presented by the partition matrix $U=\left[\gamma_{ir}\right]_{c\times m}$. The components of U must satisfy the subsequent conditions:

$$\gamma_{ir}\in[0,1]\ \ 1\le i\le c, 1\le r\le m \tag{16}$$

$$\sum_{i=1}^{c}\gamma_{ir}=1\ \ 1\le r\le m \tag{17}$$

$$0\prec\sum_{r=1}^{m}\gamma_{ir}\prec m,\ \ 1\le i\le c \tag{18}$$

It can be revealed that partition matrix (U) has c rows and m columns; c is the number of clusters, m is the number of observations. The data matrix has n rows and m columns and n is the dimension of each observation where c < n. Each element of U has a value between 0 and 1. The sum of elements on each column of U is 1.

For clustering the AE data, FCM with three clusters was applied. The number of clusters in each data set was determined due to the fact that generally within the glass/epoxy composite materials three damage mechanisms (i.e., matrix cracking, fiber/matrix debonding and fiber breakage) are common. The outcome of the analysis using three classes with different central characteristic is shown in Figure 25. The FCM results show that the AE signals are well separated along the first principal direction and are clustered in three different classes. Moreover, it can be observed from Table 4 that the AE signals distribution percentage at each cluster varies from one experimental condition to another. By considering the AE parameters of the obtained classes, the frequency parameter was best distinguished. These figures highlight three separate frequency ranges for these specimens. The lower band frequency class (class1) is the earliest damage mode that appears in the tests.

The obtained results from WPT and FCM are compared with SEM images of the damaged surfaces of the specimens and good consistency is observed between the WPT results and SEM images (Figure 26).

Table 4. Damage clustering of DCB, ENF, and MMB glass/epoxy specimens using FCM

Specimen	Percentage of each damage mechanism		
	First class (Matrix cracking)	Second class (Fiber/matrix debonding)	Third class (Fiber breakage)
GU-S1-DCB	34	30	36
GU-S1-MMB 18%	40	35	25
GU-S1-MMB 30%	55	23	22
GU-S1-ENF	60	30	10
GW-S1-DCB	49	38	13
GW-S1-MMB 18%	51	37	12
GW-S1-MMB 30%	53	37	10
GW-S1-ENF	65	27	8

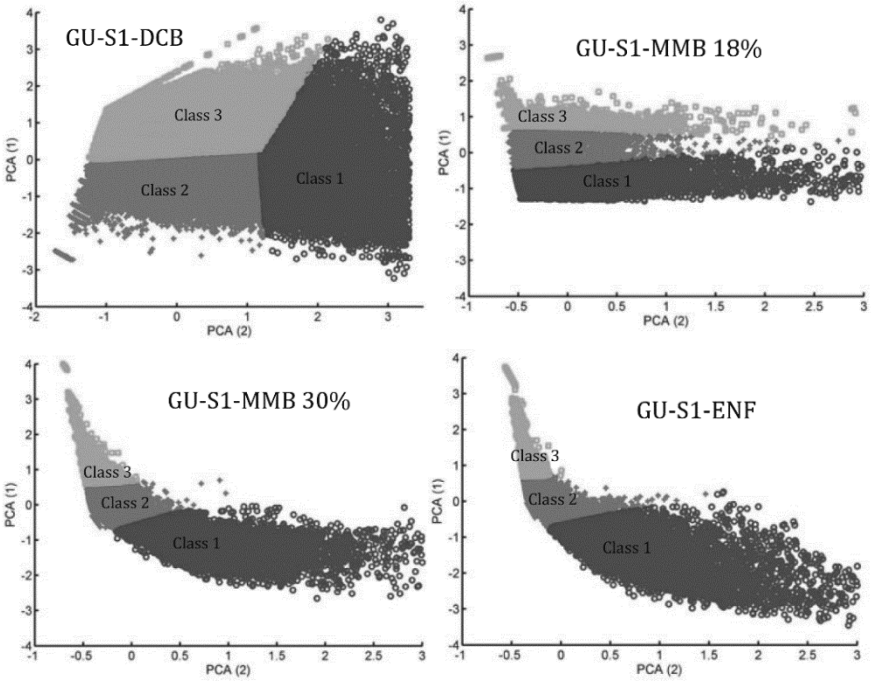

Figure 25. (Continued).

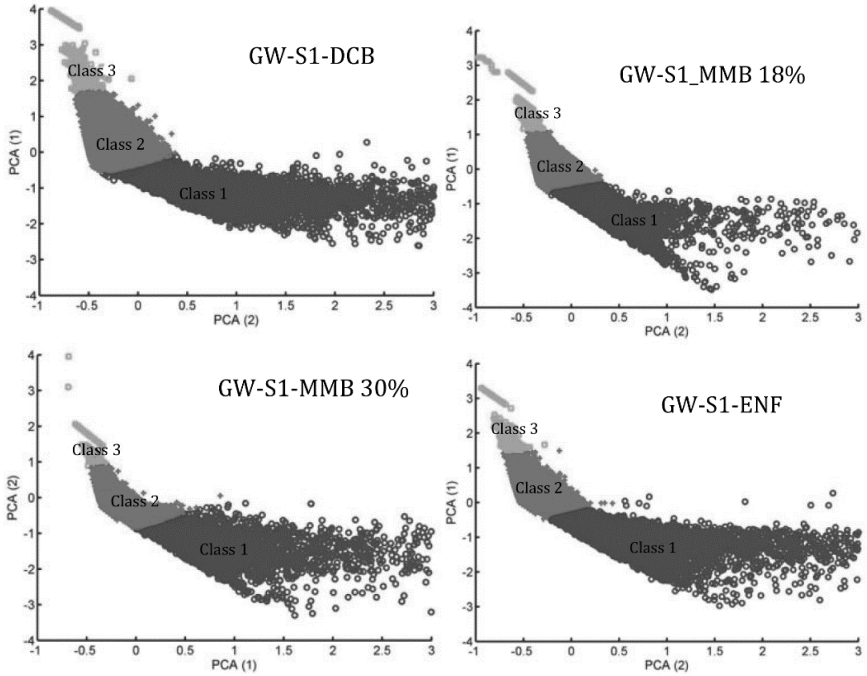

Figure 25. Damage Clustering using FCM approach.

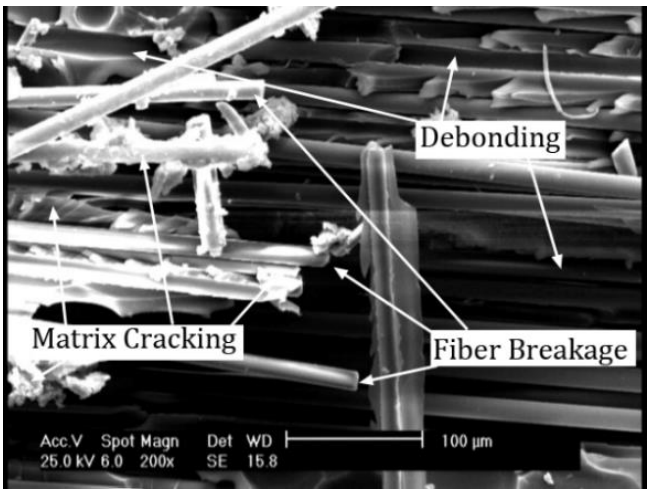

GU-S1-DCB

Figure 26. (Continued).

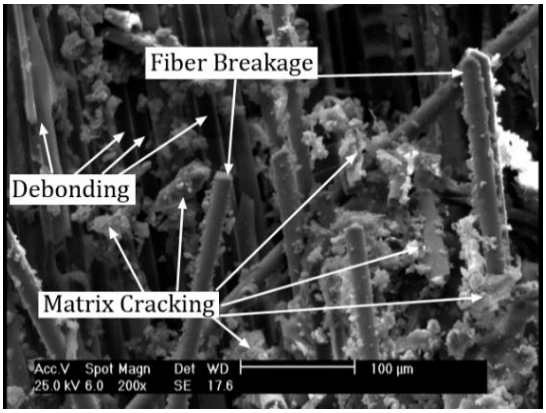

GU-S1-ENF

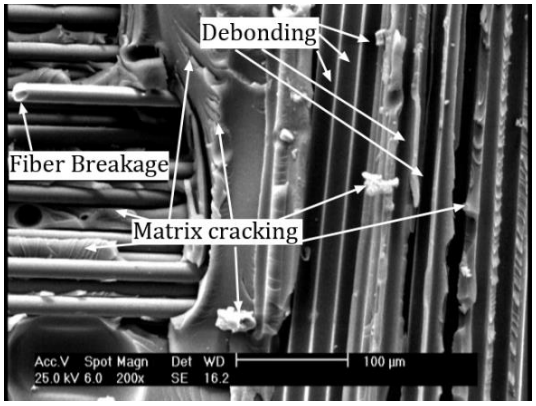

GW-S1-DCB

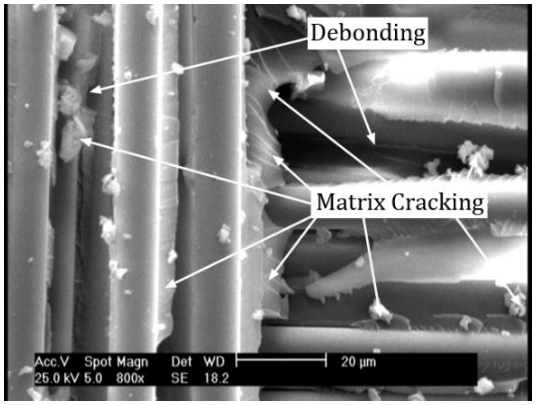

GW-S1-ENF

Figure 26. SEM images of damaged surfaces of unidirectional and woven glass/epoxy composites under different loading conditions.

CONCLUSION

This work summarizes the potential of AE technique to characterize the initiation and propagation of delamination in laminated composites. Carbon/epoxy and glass/epoxy specimens subjected to mode I (DCB), mode II (ENF), and mixed-mode I and II (MMB) loading conditions are studied. The following items are concluded.

1) The obtained results from the introduced AE methods to detect initiation of delamination, especially the Sentry function method, are shown to be more conservative than those derived from conventional fracture mechanics methodologies. This is due to the fact that AE monitoring is able to detect micro-damage mechanisms that occur before the macroscopic delamination initiation.
2) A very good agreement is achieved between the AE-predicted crack length and the actual crack length observed visually.
3) Scanning electron microscopic observations from the damaged mechanisms are in a good agreement with the AE-based classification results obtained by WPT and FCM methods. Therefore, it is concluded that the presented methods are successful in the classification process to improve the characterization of the damage mechanisms, in actual occurring modes of delamination, that is, mode I, mode II and the combination of these pure modes.
4) The SEM observations revealed that the damage mechanisms of matrix cracking, debonding, and fiber breakage were the sources of the AE signals.

REFERENCES

[1] Paris, I., and Poursartip, A. 1998. “Delamination crack tip behavior at failure in composite laminates under mode I loading.” *Journal of Thermoplastic Composite Materials* 11(1):57-69.

[2] Ho-Cheng, H., and Dharan, CKH. 1990. “Delamination during drilling in composite laminates.” *Journal of Engineering for Industry* 112(3):236-239.

[3] Fotouhi, M., and Ahmadi, M. 2014. "Acoustic emission-based study to characterize the initiation of delamination in composite materials." *Journal of Thermoplastic Composite Materials* 29(4):519-537.

[4] Tay, T.E. 2001. "Characterization and analysis of delamination fracture in composites: An overview of developments from 1990 to 2001." *Applied Mechanics Reviews* 56(1):1-32.

[5] Benzeggagh, M.L., and Kenane, M. 1996. "Measurement of mixed-mode delamination fracture toughness of unidirectional glass/epoxy composites with mixed-mode bending apparatus." *Composites Science and Technology* 56(4):439-449.

[6] Barre, S., and Benzeggagh, M.L. 1994. "On the use of acoustic emission to investigate damage mechanisms in glass-fiber reinforced polypropylene." *Composite Science Technology* 52:369-376.

[7] Bakukas, J., Prosser, W., and Johnson, W. 1994. "Monitoring damage growth in titanium matrix composites using Acoustic Emission." *Journal of Composite Materials* 28(4):305-328.

[8] Silversides, I., Maslouhi, A., and LaPlante, G. 2013. "Acoustic emission monitoring of interlaminar delamination onset in carbon fibre composites." *Structural Health Monitoring* 12(2):126-140.

[9] ASTM Standard E610-98A. 1991. "Definitions of terms relating to acoustic emission." West Conshohocken, PA: ASTM International.

[10] Miller, R.K. 1987. "Nondestructive Testing Handbook: Acoustic Emission Testing." 5th ed., American Society for Nondestructive Testing.

[11] ASTM Standard D5528. 2002. "Standard test method for mode I interlaminar fracture toughness of unidirectional fiber-reinforced polymer matrix composites." West Conshohocken, PA: ASTM International.

[12] De Kalbermatten, T., Jaggi, R., Flueler, P. et al. 1992. "Microfocus radiography studies during mode I interlaminar fracture toughness tests on composites." *Journal of material science letters* 11(9):543-546.

[13] Sridharan, S. 2008. "Delamination behaviour of composites." New York: CRC Press.

[14] Tan, P., and Tong, L. 2007. "Experimental and analytical identification of the delamination using isolated PZT sensor and actuator patches." *Journal of Composite Materials* 41(4):477-492.

[15] Benmedakhene, S., Kenane, M., and Benzeggagh, M.L. 1991. Initiation and growth of delamination in glass/epoxy composites subjected to static

and dynamic loading by acoustic emission monitoring. *Composite Science Technology* 59:201-208.

[16] Bohse, J., and Brunner, A.J. 2008. "Acoustic emission in delamination investigation. In: Sridharan S (ed.) *Delamination behaviour of composites*. New York: CRC Press, 217-277.

[17] Minak, G., and Zucchelli, A. 2008. "Damage evaluation and residual strength prediction of CFRP laminates by means of acoustic emission techniques." In: Durand LP (ed.) *Composite materials research progress*. New York: Nova Science Publishers Inc, 165-207.

[18] Saeedifar, M., Fotouhi, M., Ahmadi Najafabadi, M., Hosseini Toudeshky, H., and Minak, G. 2016. "Prediction of quasi-static delamination onset and growth in laminated composites by acoustic emission." *Composites Part B* 85:113-122.

[19] Saeedifar, M., Fotouhi, M., Ahmadi Najafabadi, M., Hosseini Toudeshky, H. 2015. "Prediction of delamination growth in laminated composites using acoustic emission and Cohesive Zone Modeling techniques." *Composite Structures* 124:120-127.

[20] Mohammadi, R., Saeedifar, M., Hosseini Toudeshky, H., Ahmadi Najafabadi, M., and Fotouhi, M. 2015. "Prediction of delamination growth in carbon/epoxy composites using a novel acoustic emission-based approach." *Journal of Reinforced Plastics and Composites* 34(11):868-878.

[21] Saeedifar, M., Ahmadi Najafabadi, M., Yousefi, J., Mohammadi, R., Hosseini Toudeshky, H., Minak, G. 2017. "Delamination analysis in composite laminates by means of Acoustic Emission and bi-linear/tri-linear Cohesive Zone Modeling." *Composite Structures* 161:505-512.

[22] ASTM E976 - 10. 2010. "Standard guide for determining the reproducibility of acoustic emission sensor response." West Conshohocken, PA: ASTM International.

[23] Wee, K.Y., Koh, S.K. and Lee, J.H. 2002. "Mode I Fracture Resistance Characteristics of Graphite/Epoxy Laminated Composites." *Polymer Composites* 21(2):155-164.

[24] de Moura, M.F.S.F., Campilho, R.D.S.G., Amaro, A.M., and Reis, P.N.B. 2010. "Interlaminar and intralaminar fracture characterization of composites under mode I loading." *Composite Structures* 92:144-149.

[25] Pereira, A.B., and de Morais, A.B. 2004. "Mode I interlaminar fracture of carbon/epoxy multidirectional laminates." *Composites Science and Technology* 64:2261-2270.

[26] Tamuzs, V., Tarasovs S., and Vilks, U. 2001. "Progressive delamination and fiber bridging modeling in double cantilever beam composite specimens." *Composites Science and Technology* 68:513-525.

[27] Fotouhi, M., Heidary, H., Ahmadi, M., and Pashmforoush, F. 2012. "Characterization of composite materials damage under quasi-static three-point bending test using wavelet and fuzzy C-means clustering." *Journal of Composite Materials* 46(15):1795-1808.

[28] Pashmforoush, F., Fotouhi, M., and Ahmadi, M. 2012. "Damage characterization of glass/epoxy composite under three-point bending test using acoustic emission technique." *Journal of Materials Engineering and Performance* 21:1380-1390.

[29] Fotouhi, M., Saeedifar, M., Sadeghi, S., Ahmadi Najafabadi, M., and Minak, G. 2015. "Investigation of the damage mechanisms for mode I delamination growth in foam core sandwich composites using acoustic emission." *Structural Health Monitoring* 14(3):265-280.

[30] Soman, K.P., and Ramachandran, K.I. 2004. "Insight into wavelets from theory to practice." India: PrenticeHall.

[31] Wojtaszczyk, P. 1997. "A mathematical introduction to wavelets." London: Cambridge University Press.

[32] Refahi Oskouei, A., Ahmadi, M., and Hajikhani, M. 2009. "Wavelet-based acoustic emission characterization of damage mechanism in composite materials under mode I delamination at different interfaces." *Express Polymer Letter* 3: 804-813.

[33] Francisco, A.T., and de Carvalho, F. 2007. "Fuzzy C-means clustering methods for symbolic interval data." *Pattern Recognition Letters* 28(4) 423-437.

[34] Sadaaki, M. 2003. "Information clustering based on fuzzy multisets." *Information Processing and Management* 39(2):95-213.

N.G.